



C-glycosyl flavone from *Urginea indica* inhibits proliferation & angiogenesis & induces apoptosis via cyclin-dependent kinase 6 in human breast, hepatic & colon cancer cell lines

Ganesh Babu Bevara, A. D. Naveen Kumar, K. Laxmi Koteshwaramma, Anil Badana, Seema Kumari & Rama Rao Malla

Department of Biochemistry, Gandhi Institute of Technology & Management (Deemed to be University), Visakhapatnam, India

Received January 12, 2016

Background & objectives: Search for novel compounds beneficial to the treatment of cancer attracts a great deal of attention. We earlier demonstrated the isolation of 5,7-dihydroxy-2-[4'-hydroxy-3'-(methoxymethyl)phenyl]-6-C- β -glucopyranosyl flavone, a novel C-glycosyl flavone from *Urginea indica* bulb. The present study was undertaken to investigate the effect of this novel compound on human normal epithelial and breast, hepatic and colon cancer cell lines.

Methods: The maximum non-toxic concentration (MNTC) and cytotoxicity of C-glycosyl flavone were assayed by 3-(4,5-dimethylthiazol-2-yl)-2,5-diphenyltetrazolium bromide (MTT). Cell cycle was analyzed by flow cytometry. Docking studies were performed to predict possible targets. Levels of cyclin-dependent kinase 1 (CDK1) and CDK6, Bcl2 and BAX and cytochrome c were quantified by specific ELISA. Mitochondrial membrane potential was determined using JC-1 dye. Apoptosis was quantified by Annexin V ELISA method.

Results: Flow cytometry analysis demonstrated G0/G1 arrest. *In silico* docking studies predicted CDK1 and CDK6 as a possible target of C-glycosyl flavone. *In vitro* study confirmed CDK6 as the main target in C-glycosyl flavone-treated cancer cell lines. C-glycosyl flavone treatment also induced membrane blebbing, chromatin fragmentation and nucleosome formation. C-glycosyl flavone treatment caused marked loss of mitochondrial membrane potential, decrease in Bcl2/BAX ratio and activation of caspase-3 and release of caspase-9 and cytochrome c. In addition, C-glycosyl flavone inhibited the tumour-induced angiogenesis and reduced the vascular endothelial growth factor levels. Similarly, CDK6 inhibitor significantly inhibited proliferation and angiogenesis and induced apoptosis in tested cell lines.

Interpretation & conclusions: The results indicate that C-glycosyl flavone may exert induction of apoptosis, cell cycle arrest and inhibition of angiogenesis via CDK6. Thus, targeting CDK6 using C-glycosyl flavone may serve as a novel therapeutic approach for the treatment of breast, hepatic and colon cancers.

Key words Angiogenesis - apoptosis - cell cycle - C-glycosyl flavone - *Urginea indica*

Cyclin-dependent kinases (CDKs) play a vital role in the cell cycle control, apoptosis, transcription and neuronal functions. In particular, CDKs that promote transition through the cell cycle are expected to be a key therapeutic target because many tumorigenic events ultimately enhance proliferation by impinging on CDK6 complexes in the G1 phase of the cell cycle¹. Expression and interaction of cyclins, CDKs and their activators or inhibitors correlate with the timing of events in the cell cycle². In addition, a kinase-independent function of CDK6 regulates tumour angiogenesis through transcription of vascular endothelial growth factor (VEGF) and P16^{INK4A} by interacting with STAT and AP-1³. There is a role of CDK6 in DNA-binding complex that binds DNA in an androgen receptor-dependent manner to enhance the transcription of prostate-specific antigen⁴. A variety of naturally occurring compounds, including flavonoids, alkaloids and terpenoids or their derivatives, have been found to be CDK inhibitors⁵.

The flavonoids are a highly diverse class of polyphenolic compounds formed principally as secondary metabolites with broad functional roles *in planta*. These may occur as glycosylated compounds with C-C bond between sugar moiety and flavonoid skeleton. C-glycosyl flavones are stable and less explored sub-class of glycosyl flavonoids of medicinal plants⁶. These possess many important biological activities including antimicrobial, antioxidant and hepatoprotective activities⁷. The C-glycosyl flavonoids exhibit higher antioxidant and anti-diabetes potential than their corresponding O-glycosyl flavonoids and aglycones⁸. However, limited information is available in the literature regarding the anticancer activity of C-glycosyl flavone.

Urginea indica is commonly called as sea onion and its bulbs have been used to cure wounds and infections⁹. Antimicrobial, anti-inflammatory, antioxidant and cytotoxic activities of *U. indica* have been reported elsewhere^{10,11}. Deepak and Salimath¹² reported a novel glycoprotein with anti-angiogenic and pro-apoptotic activity. Sultana *et al*¹³ reported O-glycosyl flavone and flavonone in the bulb. However, the search for novel compounds that could be beneficial for the treatment of cancer is continued. We have earlier reported the C-glycosyl flavone in the bulb of *U. indica*¹⁴. The objective of this study was to evaluate the maximum non-toxic concentration (MNTC) against human normal breast epithelial cell line (MCF-12A) and anticancer activity against human breast carcinoma

cell line (MCF-7), hepatocellular carcinoma cell line (Hep-G2) and colon cancer cell line (HT-29), in terms of proliferation, angiogenesis and apoptosis.

Material & Methods

All solvents were obtained from Merck, Mumbai, India. 3-(4,5-dimethylthiazol-2-yl)-2,5-diphenyltetrazolium bromide (MTT) reagent was purchased from Sigma, USA. MCF-7, Hep-G2 and HT-29 cell lines were obtained from National Centre for Cell Sciences, Pune, India, and MCF-12A was purchased from ATCC, USA. Cell lines were grown in minimal essential medium (MEM) with 10 per cent foetal bovine serum (FBS), 100 units of each penicillin and streptomycin at 37°C in 5 per cent CO₂ incubator. The present study was carried out during the period 2013-2015, in the Cancer Biology Laboratory, Department of Biochemistry, GITAM Institute of Science, GITAM (Deemed to be University), Visakhapatnam, India.

Isolation and characterization of C-glycosyl flavonoids: Silica gel column chromatography was performed for the isolation of C-glycosyl flavone from the methanolic extract of *U. indica* bulb using methanol and ethyl acetate as the solvent system (60:40 v/v). The structure was elucidated based on infrared (IR), nuclear magnetic resonance (NMR) and mass spectral data¹⁴.

Maximum non-toxic concentration (MNTC): A preformed monolayer of MCF-12A cells in a 96-well plate (1×10⁴ cells/well) was treated with C-glycosyl flavone at 2, 4, 8, 16, 32, 64, 128, 256 and 512 µg/ml for 48 h and MNTC was determined by *in vitro* cytotoxicity assay using MTT¹⁵. Cell and nuclear morphologies were also observed.

MTT assay: The cytotoxic activity of isolated C-glycosyl flavone [2, 4, 8, 16, 32, 64 and 128 µg/ml (MNTC)] against MCF-7, HT-29 and Hep-G2 cells (1×10⁴) was determined using MTT assay. 5-fluorouracil (5-FU) and tamoxifen were used as positive controls. The concentration required to reduce 50 per cent viability (IC₅₀) was calculated by regression analysis¹⁶.

Cell cycle analysis: Cells in 6-well plate (1×10⁶ cells/well) were treated with C-glycosyl flavone at an approximate growth inhibition concentration-50 (25 µg/ml) for 48 h and the cell cycle was analyzed by Flow Cytometry (BD Accuri C6, USA)¹⁷.

Computation of docking scores using PatchDock: The crystal structures of CDKs were retrieved from the

Protein Data Bank (<http://www.rcsb.org/pdb/home/home.do>). The IDs were as follows: 4CFM, 1HCK, 2WIH, 2W99, 1H4L and 4AUA. The two-dimensional (2D) structure of isolated C-glycosyl flavone was designed and converted to 3D structure using ACD-ChemSketch Software (ACD/ChemSketch, Version 12, Advanced Chemistry Development, Inc., Toronto, ON, Canada, www.acdlabs.com, 2015). The Lipinski's property of C-glycosyl flavone was computed¹⁸. The 3D structure of CDK1, CDK2, CDK3, CDK4, CDK5 and CDK6 and C-glycosyl flavone was submitted to PatchDock Server (<http://bioinfo3d.cs.tau.ac.il/PatchDock>) and the results were evaluated for active site interactions by UCSF-Chimera Software¹⁹.

Quantification of CDK1 and CDK6 using ELISA: Quantification of CDK1 and CDK6 was performed using the ELISA method. Treated and untreated cell lysates were normalized with reference to total protein. The normalized volumes were added to CDK1- or CDK6-specific antibody-coated wells and incubated for 2 h at 37°C as per the manufacturer's instructions (Antibodies, Atlanta, USA). The quantity of CDK1 or CDK6 in C-glycosyl flavone-treated cells was determined and expressed as per cent control.

Morphological assessment of cell apoptosis: Cells in 4-well chamber slide (1×10^4 cells/well) were treated with C-glycosyl flavone at 25 µg/ml for 72 h, stained with 50 µl of Hoechst 33342 (100 µg/ml) for 15 min and images were captured at a wavelength of 461 nm using a fluorescence-inverted microscope (Olympus, Japan).

Mitochondrial membrane potential assay: Briefly, cells in 6-well plate (1×10^6 cells/well) were treated with C-glycosyl flavone at 25 µg/ml for 72 h and stained with 500 µl of 200 µM JC-1 for 20 min at 37°C. The fluorescence of the cell suspension was measured using a microplate reader at Ex/Em(green)/Em(red)::485/538/590nm²⁰.

Assay for chromatin fragmentation accompanying cell death: The cell death induced by C-glycosyl flavone (25 µg/ml) was detected with the cell death ELISA kit (Boehringer-Mannheim, Germany). The DNA-histone complexes generated during apoptotic DNA fragmentation were measured as per the manufacturer's instructions. Absorbance at 405 nm was measured using a microplate reader, and the results

were expressed as an enrichment factor relative to the untreated controls.

Assay for annexin V accompanying cell death: C-glycosyl flavone-induced apoptosis in cancer cells was quantified using Annexin V ELISA method. Briefly, cells in 96-well plate (1×10^4 cells/well) were treated with C-glycosyl flavone at 25 µg/ml for 72 h. Then, 50 µl of annexin V antibody was added and incubated at 25°C for 1 h. The apoptosis rate was determined as per the manufacturer's instructions (Abcam, USA).

Assay of Bcl2 and BAX by ELISA: Cells (5×10^6 cells/ml) were treated with C-glycosyl flavone (25 µg/ml) for 72 h. The cell lysate (50 µl) and 50 µl of antibody specific to either Bcl2 or BAX were added to each well and incubated at room temperature for 1 h. The Bcl2 or BAX levels were measured using specific kit (Abcam, USA).

Measurement of caspase-3 and caspase-9 activity: The activity of caspase-3 or caspase-9 was determined using a colorimetric assay according to the manufacturer's instructions (Chemicon International Inc., USA). After 72 h of treatment, cell lysates were treated with peptide substrate conjugated with Ac-DEVD-pNA for caspase-3 and Ac-LEHD-AFC for caspase-9. After overnight incubation, optical density was measured at 405 nm using a microplate reader.

Assay for cytochrome c release: The treated and untreated cell lysates were normalized to total protein. The normalized volumes were added to the cytochrome c-specific antibody-coated 96-well plate along with biotinylated cytochrome c detection antibody and incubated for 2 h at room temperature. Cytochrome c in cell lysates was measured using human cytochrome c ELISA kit (Abcam, USA) as per the manufacturer's instructions.

Capillary formation assay: An *in vitro* capillary tube formation assay was performed as described earlier²¹. Briefly, human umbilical vein endothelial cells (1×10^4) were plated onto a matrigel-coated 4-well chamber slide and incubated with conditioned medium from untreated or C-glycosyl flavone-treated (25 µg/ml) cells. After overnight incubation, the slide was examined and photographed²¹. Total tube length was determined using image analysis software (Image J; NIH, Bethesda, MD, USA).

Quantification of vascular endothelial growth factor (VEGF) levels: The lysate (10 µl) from untreated/treated

cells was incubated overnight at 4°C in a 96-well plate. The VEGF levels were determined using ELISA as per the manufacturer's instructions (Thermo Scientific, USA).

Statistical analysis: The experiments were carried out three times separately and the data were expressed as mean \pm standard deviation. Statistical differences between untreated and treated cells were determined using one-way ANOVA. IC₅₀ value was calculated using regression analysis.

Results

MNTC of isolated C-glycosyl flavones: The isolated C-glycosyl flavone was used for evaluation of anticancer activity (Fig. 1A). In the present investigation, the MNTC of isolated C-glycosyl flavone towards the human normal breast epithelial cell line MCF-12A as evaluated using MTT assay was 128 μ g/ml (Fig. 1B) without any visible effect on the cell and nuclear morphology (Fig. 1C and D) of MCF-12A cells.

Treatment with C-glycosyl flavone inhibits proliferation of cancer cells: As a preliminary study, the anti-proliferative activity of isolated C-glycosyl flavone was evaluated using MTT assay and cell cycle analysis against MCF-7 which served as an excellent *in vitro* model for studying the mechanism of tumour response. MCF-7 cells exhibited low acidification and

high respiratory rate. HT-29 and Hep-G2 were easy to handle and retained many of the morphological characteristics. The percentage of antiproliferative activity of C-glycosyl flavone against MCF-7, HT-29 and Hep-G2 cells was compared to control and is plotted in Fig. 2A. However, the tamoxifen standards against MCF-7 (Fig. 2B) and the 5-FU against HT-29 cells (Fig. 2C) and Hep-G2 (Fig. 2D) were determined at a concentration of 2, 4, 8, 16, 32, 64 and 128 μ g/ml. The results demonstrated C-glycosyl flavone mediated concentration-dependent decline in the MCF-7, HT-29 and Hep-G2 cell proliferation versus untreated control. The IC₅₀ values of C-glycosyl flavone against MCF-7, Hep-G2 and HT-29 cells was 29.60, 26.87 and 15.10 μ g/ml, respectively. However, IC₅₀ value of tamoxifen against MCF-7 was 1.94 μ g/ml and of 5-FU against HT-29 and Hep-G2 was 1.87 and 1.76 μ g/ml, respectively. The results of cell cycle analysis showed that C-glycosyl flavone treatment at an approximate growth inhibition concentration-50 (Gi-50) (25 μ g/ml) for 48 h induced an increase of G0/G1 phase cells from 58.48 to 71.04 per cent and a decrease of S phase population from 20.88 to 12.02 per cent and G2/M phase cells from 14.64 to 7.94 per cent in MCF-7 (Fig. 2E). In HT-29, G0/G1 cells increased from 58 to 72.44 per cent, while S phase and G2/M phase cells decreased from 23.12 to 12.2 per cent and 14.88 to 5.36 per cent, respectively (Fig. 2F). In case of

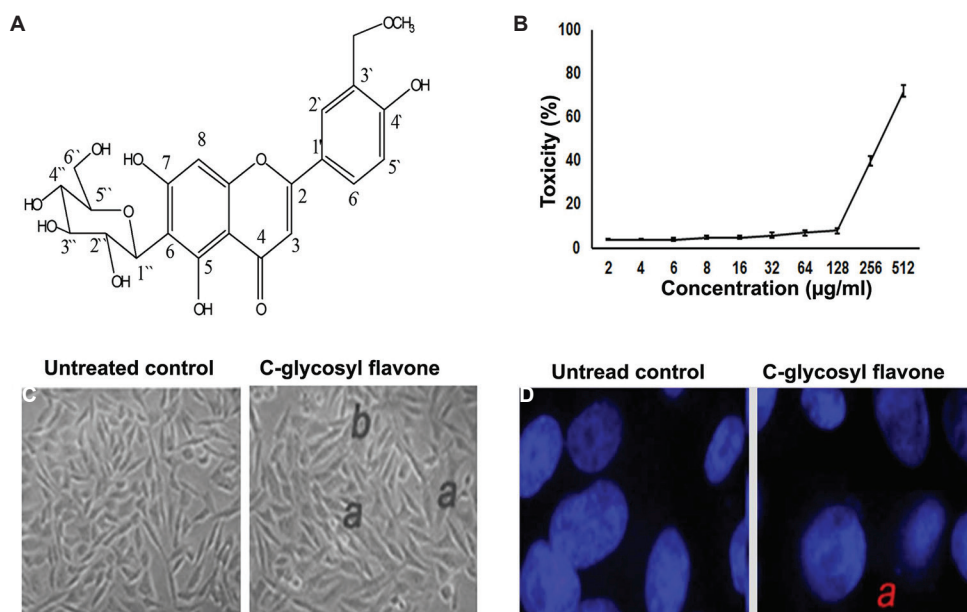


Fig. 1. Non-toxic effect of C-glycosyl flavone isolated from *Urginea indica* bulb. (A) Structure of C-glycosyl flavone. (B) Cytotoxic effect of C-glycosyl flavone on normal breast epithelial cell line, MCF-12A cells. The values are represented as percentage of toxicity. (C) Morphological changes using ($\times 20$) magnification phase-contrast microscope (a) early apoptotic cells and (b) viable cells. (D) Nuclear changes using Hoechst 33258 stain using fluorescent microscope ($\times 40$).

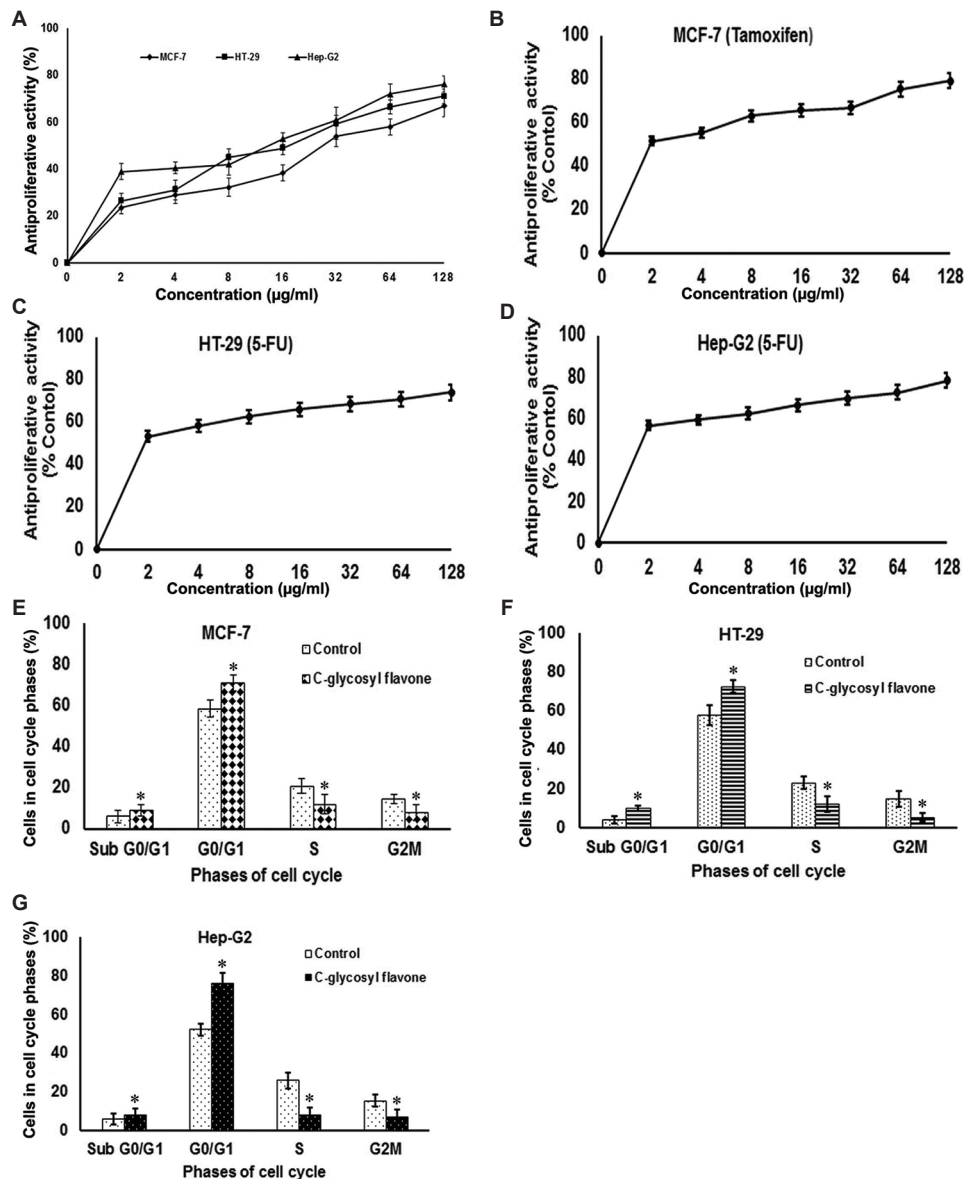


Fig. 2. Anti-proliferative activity of C-glycosyl flavone (A) against MCF-7, Hep-G2 and HT-29 cell lines, (B) tamoxifen against MCF-7, (C) 5-fluorouracil against HT-29 and (D) Hep-G2. (E) Effect of C-glycosyl flavone on cell cycle phases of MCF-7, (F) HT-29 and (G) Hep-G2 using flow cytometer. The values are represented as % of cell population. Each value represents mean±standard error of three independent experiments. * $P < 0.05$ compared to control.

Hep G2 cells, G0/G1 population increased from 52.4 to 76.44 per cent, while S phase and G2/M phase cells decreased from 26 to 8.2 per cent and 15.6 to 7.36 per cent, respectively (Fig. 2G).

The CDKs and their regulatory proteins, cyclins, play an important role in the transition of the cell cycle from quiescence (G0) to proliferating stage. The docking of C-glycosyl flavone with CDKs was scored based on their complementarity and rank ordered. C-glycosyl flavone exhibited significant

score with CDK6 (7092) followed by CDK1 (7010), CDK3 (6560), CDK5 (6434), CDK4 (6378) and CDK2 (5978) (Fig. 3A-F). Based on high rank-ordered score, the CDK1 and CDK6 were chosen for further study. The effect of C-glycosyl flavone on CDK1 and CDK6 in cancer cell lines was evaluated using ELISA. The concentration of CDK6 in untreated MCF-7, HT-29 and Hep-G2 cells was 8.8, 8.7 and 8.8 ng/ml as against 5.8, 6.0 and 5.2 ng/ml, respectively, in corresponding C-glycosyl flavone-treated cell. Thus, CDK6 activity in C-glycosyl flavone-treated cells was decreased

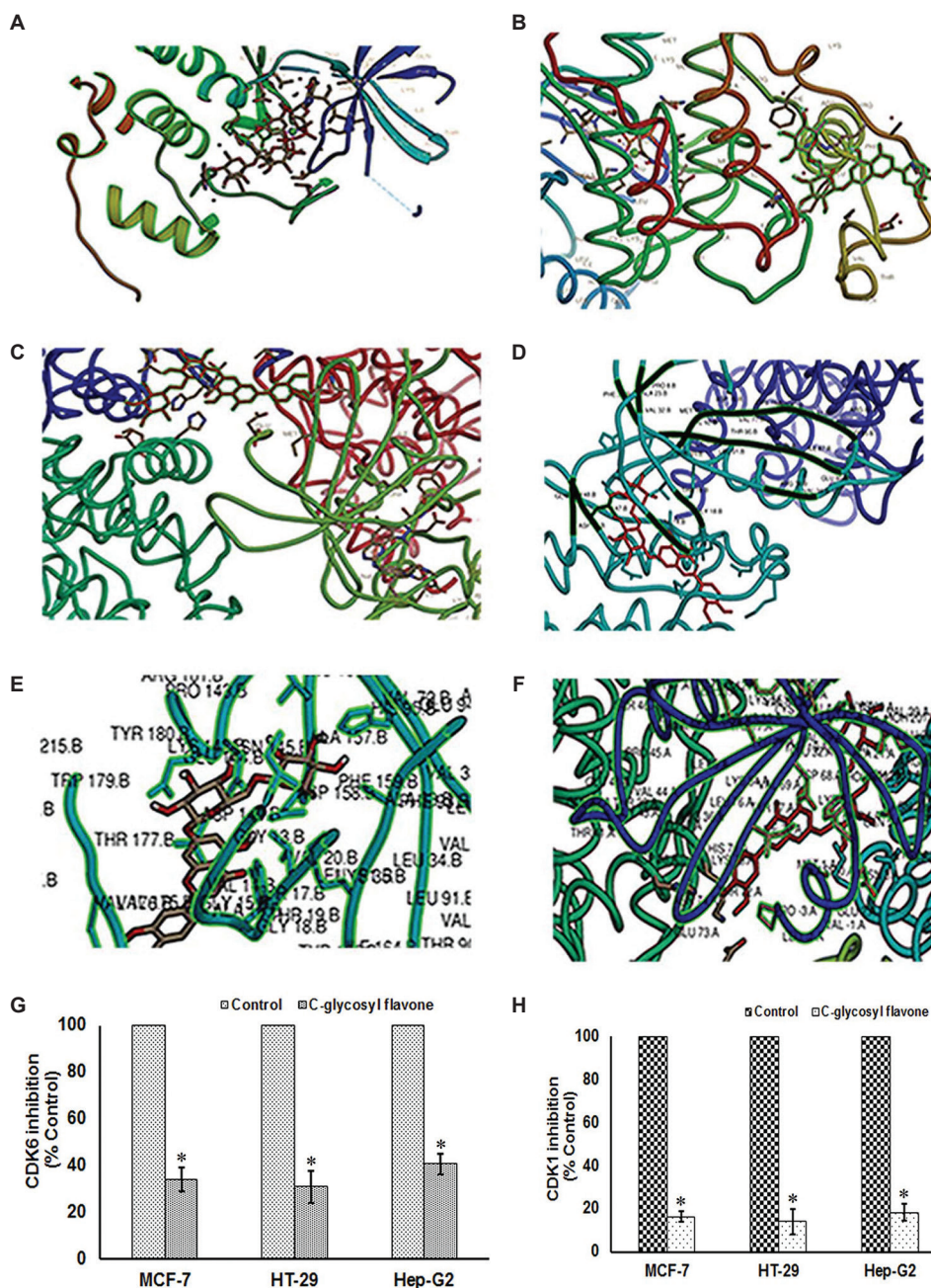


Fig. 3. Molecular docking of cyclin-dependent kinases (CDKs) with C-glycosyl flavone. Docking pose was (A) CDK1, (B) CDK2, (C) CDK3, (D) CDK4, (E) CDK5, (F) CDK6 with docking score of 7010, 5978, 6560, 6378, 6434 and 7092, respectively, using PatchDock. The scores were based on hydrophilic, Van der Waals interactions and hydrogen bonding interactions. (G and H) CDK1 and CDK6 levels were determined using ELISA assay expressed as percentage control. Each value represents mean±standard error of three independent experiments. * $P < 0.05$ compared to control.

34.1 per cent in MCF-7, 31.03 per cent in HT-29 and 40.9 per cent in Hep-G2 cells compared to control (Fig. 3G). The concentration of CDK1 in control and C-glycosyl flavone-treated cells was 8.6 and 7.2 ng/ml for MCF-7 cells, 8.5 and 7.3 ng/ml for HT-29 cells and 8.7 and 7.1 ng/ml for Hep-G2 cells, respectively. CDK1 decreased by 16.3 per cent in MCF-7, 14.1 per cent

in HT-29 and 18.4 per cent in Hep-G2 cells following C-glycosyl flavones treatment (Fig. 3H).

Treatment with C-glycosyl flavone induces apoptosis in human cancer cells: The observation of cell morphology under phase-contrast microscope demonstrated that C-glycosyl flavone treatment at

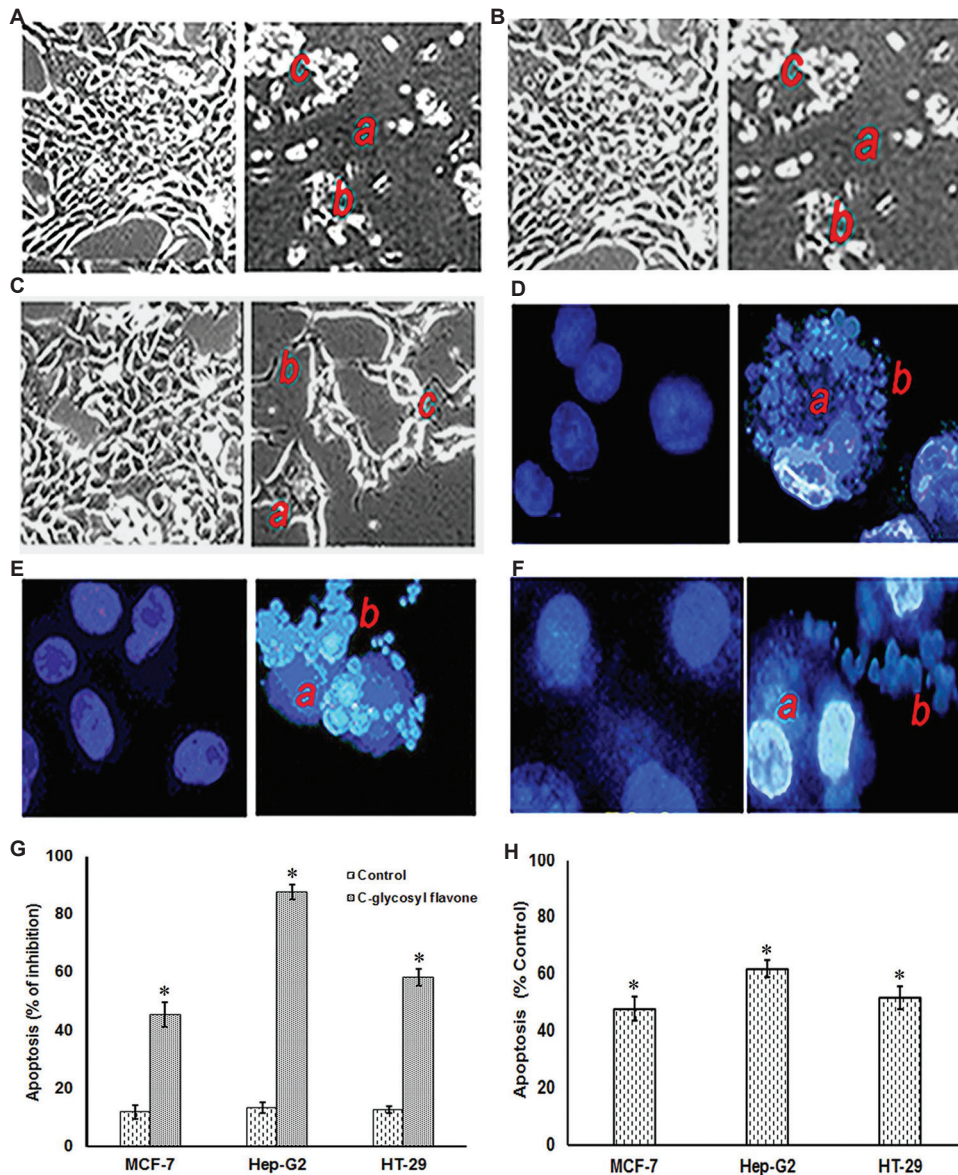


Fig. 4. C-glycosyl flavone-induced apoptotic changes were viewed ($\times 20$). (A) MCF-7, (B) Hep-G2 and (C) HT-29 at 25 $\mu\text{g/ml}$ treatment compared to untreated control cells. Cells at different stages of apoptosis have been specified as (a-cell shrinkage; b-blebbing; c-loss of cell adhesion). Nuclear changes viewed under fluorescent microscope ($\times 40$) using Hoechst 33258 stain. (D) MCF-7, (E) Hep-G2 and (F) HT-29 cells. (G) Effect of C-glycosyl flavone treatment for 72 h on cell death (H) was evaluated. Each value represents mean \pm standard error of three independent experiments. * $P < 0.05$ compared to control.

25 $\mu\text{g/ml}$ for 72 h significantly induced cell shrinkage, blebbing of the membrane and loss of cell adhesion in Hep-G2 followed by HT-29 and MCF-7 (Fig. 4A-C). These modifications are the characteristics of the apoptotic cells. Further, C-glycosyl flavone strongly induced the nuclear condensation and formation of apoptotic bodies in the same order compared to untreated controls (Fig. 4D-F).

Compared to untreated controls, exposure of MCF-7, HT-29 and Hep-G2 cells to C-glycosyl flavone

at 25 $\mu\text{g/ml}$ for 72 h resulted in 3.8-, 4.6- and 6.5-fold increase in the induction of apoptosis, respectively (Fig. 4G). Annexin V staining of C-glycosyl flavone treated MCF-7, HT-29 and Hep-G2 cells showed 48, 52 and 62 per cent apoptosis, respectively, compared to controls (Fig. 4H). Loss of mitochondrial membrane potential is a prerequisite for mitochondrial-mediated apoptosis. The C-glycosyl flavone caused 53, 64 and 71 per cent loss of mitochondrial membrane potential in MCF-7, HT-29 and Hep-G2 cells, respectively, corresponding to controls (Fig. 5A).

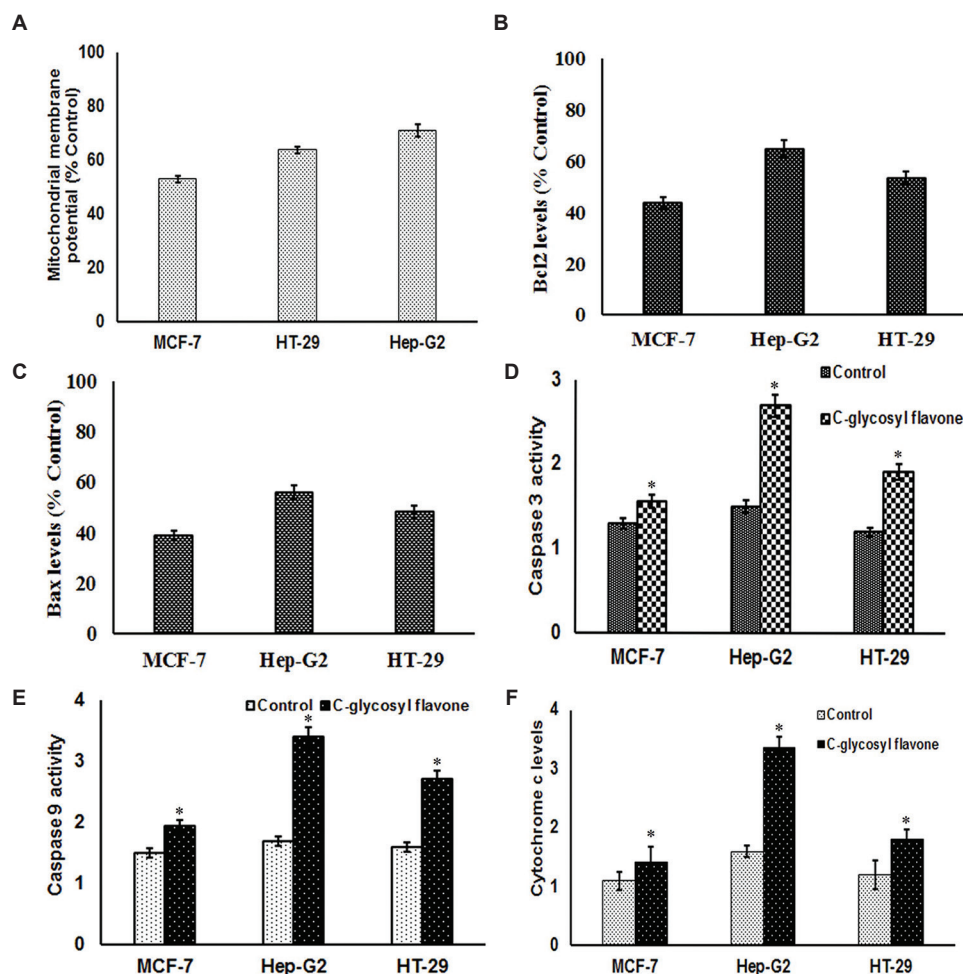


Fig. 5. Effect of C-glycosyl flavone on mitochondrial-mediated apoptosis. (A) Effect of C-glycosyl flavone (25 µg/ml) on mitochondrial membrane potential. Effect of C-glycosyl flavone (25 µg/ml) on (B) Bcl2 and (C) BAX levels compared to percentage control. Effect of C-glycosyl flavone (25 µg/ml) on the activity of (D) caspase-3 and (E) caspase-9. (F) Effect of C-glycosyl flavone (25 µg/ml) on cytochrome c levels. Each value represents mean±standard error of three independent experiments. * $P < 0.05$ compared to control.

In the present study, treatment of MCF-7, HT-29 and Hep-G2 cells with C-glycosyl flavone decreased the Bcl2 protein levels by 43.6, 53.2 and 64.8 per cent, respectively, compared to controls (Fig. 5B). However, BAX levels seemed to increase by 38.6, 48.4 and 55.8 per cent, respectively, compared to controls (Fig. 5C). To confirm the effect of C-glycosyl flavone on apoptosis, the activity of caspase-3 and caspase-9, the biochemical markers of apoptosis was determined. It was found that C-glycosyl flavone (25 µg/ml) increased caspase-3 activity by 1.2, 1.6 and 1.8 folds and caspase-9 by 1.3, 1.7 and 2 folds in MCF-7, HT-29 and Hep-G2 cell lysates, respectively, compared to untreated control (Fig. 5D and E). The release of cytochrome c from apoptotic cells triggers sequential maturation of caspase-9 and caspase-3 in caspase-dependent cell death events. Therefore, the effect of C-glycosyl flavone on cytochrome c levels was

determined. C-glycosyl flavone at 25 µg/ml increased the release of cytochrome c by 1.3, 1.5 and 2.1 folds in MCF-7, HT-29 and Hep-G2 cells, respectively, compared to untreated controls (Fig. 5F).

Treatment with C-glycosyl flavone decreased tumour-induced capillary formation in human cancer cells: To analyze the effect of C-glycosyl flavone on tumour-induced angiogenesis, total capillary formation and VEGF levels were determined. It was observed that C-glycosyl flavone (25 µg/ml) decreased the capillary formation by 32, 43 and 48 per cent in MCF-7, HT-29 and Hep-G2 cells, respectively, compared to untreated controls (Fig. 6A). Further, VEGF levels were decreased by 38, 47 and 53 per cent in MCF-7, HT-29 and Hep-G2 cells, respectively, compared to untreated controls (Fig. 6B).

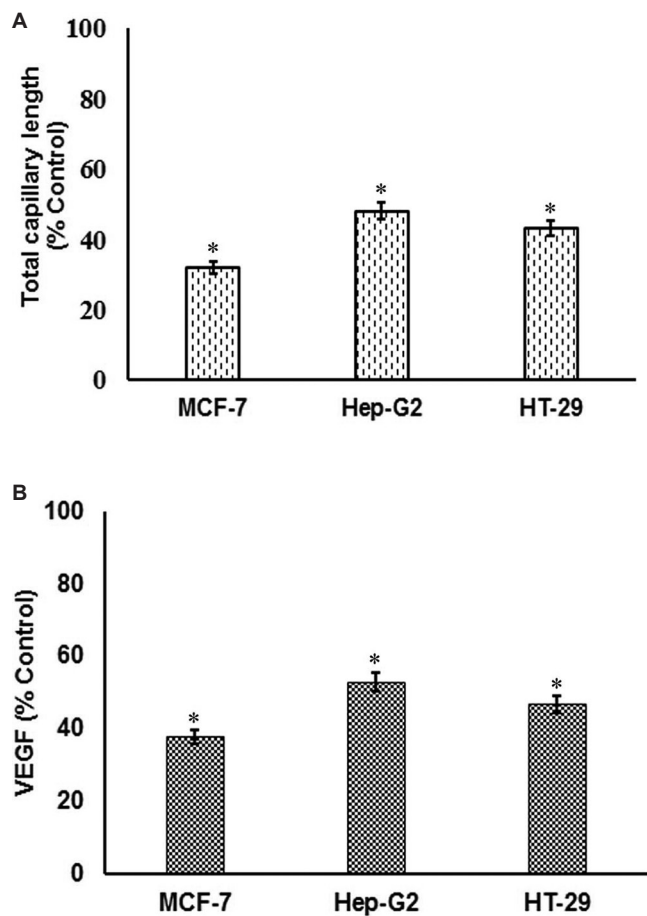


Fig. 6. Effect of C-glycosyl flavone on tumour-induced capillary formation. (A) Effect of C-glycosyl flavone (25 µg/ml) on tumour-induced angiogenesis in terms of total capillary length. (B) Effect of C-glycosyl flavone (25 µg/ml) on vascular endothelial growth factor (VEGF) levels was evaluated and values represented compared to percentage control). Each value represents mean±standard error of three independent experiments. * $P < 0.05$ compared to control.

Discussion

During the cytotoxicity screening, it was found that C-glycosyl flavone exhibited significantly high MNTC (128 µg/ml) against MCF-12A cells. According to the US National Cancer Institute screening cell line programme²², the drug with IC_{50} value ≤ 25 µg/ml is considered as efficient anticancer drug. Accordingly, the C-glycosyl flavone can be considered as an effective anticancer agent against Hep-G2 (IC_{50} : 15.3 µg/ml) and HT-29 (IC_{50} : 24.2 µg/ml) cells, but moderately effective agent against MCF-7 breast cancer cells (IC_{50} : 28 µg/ml)²³.

In the present study, an increased G1/Go phase and decreased S phase population were noticed with C-glycosyl flavone at approximate growth inhibitory

concentration-50 (25 µg/ml), which could be due to arrest of cell cycle at G1/Go phase. Further, a decrease in the S phase population indicates a reduced cell division. CDKs are fundamental in cell cycle control²⁴. The CDKs with their respective regulatory partner cyclin are involved in the regulation of the cell cycle, apoptosis and transcription. In this study, based on good binding affinity of C-glycosyl flavone in docking, CDK1 and CDK6 appeared to be its probable targets. Earlier, inhibition of CDK6 activity by flavonoid inhibitors such as fisetin, apigenin and chrysin was evaluated using computational approaches²⁵. In this study, significant inhibition of CDK6 was observed in cancer cell lines targeted with C-glycosyl flavone. Targeting CDK6 by flavopiridol, a flavonoid derivative, was reported in cancer cell lines²⁶. Earlier, Cover *et al*²⁷ reported that inhibition of CDK6 activity closely related to the reduction of cell proliferation in human breast cancer cells.

Apoptosis is the most common mechanism of action of chemotherapeutic agents, including natural products. After 72 h of treatment with C-glycosyl flavone, increased DNA fragmentation was observed as hallmarks of apoptosis²⁸. The apoptotic changes in cancer cells induced by C-glycosyl flavone were evaluated using antibody-based assay. DNA fragmentation and release of nucleosomes into the cytoplasm in C-glycosyl flavone-treated cancer cells suggested induction of apoptosis. The characteristics of the apoptotic cells such as cell shrinkage, membrane blebbing, loss of cell adhesion, nuclear condensation and cell fragmentation were observed with C-glycosyl flavone after 72 h treatment in all tested cancer cell lines but more significantly in Hep-G2. As C-glycosyl flavone triggered apoptosis in tested cancer cell lines at 72 h, it may be recognized as an anticancer drug²⁹.

Mitochondria are known to play a central role in the apoptotic process³⁰. A significant loss of mitochondrial membrane potential with C-glycosyl flavone showed mitochondrial-mediated apoptosis. This study demonstrated decreased Bcl-2 level and marginally increased Bax levels with Bax/Bcl-2 ratio in C-glycosyl flavone-treated Hep-G2, HT-29 and MCF-7 cells compared to controls. The flavopiridol, synthetic flavone and CDK inhibitor down-regulated Bcl-2 and induced growth arrest and apoptosis in chronic B-cell leukaemia lines³¹. Our results also showed that the change of Bax/Bcl-2 ratio might be a key factor in inducing apoptosis in cancer cells.

The intrinsic pathway of apoptosis is characterized by mitochondrial dysfunction with the release of cytochrome c, activation of caspase-9 and subsequently of caspase-3³². Increased caspase-3 and caspase-9 activities and chromatin condensation, apoptotic body formation and DNA fragmentation may be the underlying mechanism of C-glycosyl flavone-induced apoptosis in cancer cells.

Angiogenesis, a highly complex process involving multiple interactions of pro- and anti-angiogenic factors, is required to supply nutrients and oxygen to sustain the tumours. VEGF is the predominant regulator of tumour angiogenesis²¹. VEGF can be upregulated by oncogene expression, growth factors and hypoxia. Flavonoids have been proposed to act as chemopreventive agents based on epidemiological studies. They have been shown to inhibit angiogenesis and proliferation of tumour cells and endothelial cells³³. Glycosyl flavones are known to inhibit proliferation as well as angiogenesis³⁴. However, the association of C-glycosyl flavone with angiogenesis is not clear. A significant inhibition of tumour-induced capillary formation and reduced expression of VEGF was noticed in C-glycosyl flavone-treated cancer cell lines.

The limitation of our study was that anticancer activity of C-glycosyl flavone was tested only in breast (MCF-7), hepatic (Hep-G2) and colon (HT-29) cancers.

In conclusion, the mechanism of anticancer activity of C-glycosyl flavone against MCF-7, HT-29 and Hep-G2 may involve blockage of cell cycle, inhibition of angiogenesis and induction of apoptosis probably through inhibition of CDK6. Thus, targeting CDK6 using C-glycosyl flavone may serve as a novel therapeutic strategy for the treatment of breast, hepatic and colon cancers.

Financial support & sponsorship: Authors thank the Department of Science and Technology (DST), New Delhi, India for financial support as DST-SERB (No: SR/SO/BB-0091/2012 dated 20-06-2013) and DST-FIST.

Conflicts of Interest: None.

References

- Asghar U, Witkiewicz AK, Turner NC, Knudsen ES. The history and future of targeting cyclin-dependent kinases in cancer therapy. *Nat Rev Drug Discov* 2015; 14 : 130-46.
- Joshi KS, Rathos MJ, Joshi RD, Sivakumar M, Mascarenhas M, Kamble S, *et al.* *In vitro* antitumor properties of a novel cyclin-dependent kinase inhibitor, P276-00. *Mol Cancer Ther* 2007; 6 : 918-25.
- Kollmann K, Heller G, Schneckenleithner C, Warsch W, Scheicher R, Ott RG, *et al.* A kinase-independent function of CDK6 links the cell cycle to tumor angiogenesis. *Cancer Cell* 2013; 24 : 167-81.
- Lim JTE, Mansukhani M, Weinstein IB. Cyclin-dependent kinase 6 associates with the androgen receptor and enhances its transcriptional activity in prostate cancer cells. *Proc Natl Acad Sci U S A* 2005; 102 : 5156-61.
- Khan MTH, Ather A. Editors. *Lead molecules from natural products: Discovery and new trends*. Vol. 2, 1st edition. Amsterdam: Elsevier Science; 2006. p. 157-69.
- Zeng P, Zhang Y, Pan C, Jia Q, Guo F, Li Y, *et al.* Advances in studying of the pharmacological activities and structure - Activity relationships of natural C-glycosyl flavonoids. *Acta Pharm Sin B* 2013; 3 : 154-62.
- Chelyn JL, Omar MH, Mohd Yousof NS, Ranggasamy R, Wasiman MI, Ismail Z, *et al.* Analysis of flavone C-glycosides in the leaves of *Clinacanthus nutans* (Burm. f.) lindau by HPTLC and HPLC-UV/DAD. *ScientificWorldJournal* 2014; 2014 : 724267.
- Xiao J. Phytochemicals in food and nutrition. *Crit Rev Food Sci Nutr* 2016; 56 (Suppl 1): S1-3.
- Deb DBDS. Studies on Indian squill – *Urginea indica* (Roxb.) Kunth. *Q J Crude Drug Res* 1976; 14 : 49-60.
- Rahman MM, Chowdhury JA, Habib R, Saha BK, Razibul Habib, Saha BK, *et al.* Anti-inflammatory, anti-arthritic and analgesic activity of the alcoholic extract of the plant *Urginea indica* Kunth. *IJPSR* 2011; 2 : 2915-9.
- Bevara GB, Kumar ADN, Rao DB, Koteswaramma KL, Pakalapati S, Malla RR. Analysis of antioxidant and anticancer potentials of *Urginea indica*, an endangered medicinal plant. *Sect Title Pharmacol* 2012; 5 : 4921-8.
- Deepak AV, Salimath BP. Antiangiogenic and proapoptotic activity of a novel glycoprotein from *U. indica* is mediated by NF-kappaB and caspase activated DNase in ascites tumor model. *Biochimie* 2006; 88 : 297-307.
- Sultana N, Akter K, Nahar N, Khan MS, Mosihuzzaman M, Sohrab MH, *et al.* Novel flavonoid glycosides from the bulbs of *Urginea indica* Kunth. *Nat Prod Res* 2010; 24 : 1018-26.
- Babu BG, Kumar ADN, Badana A, Kumari S, Jha A, Malla R. Effect of C-glycosyl flavone from *Urginea indica* on antibiotic induced microbial cell death. *Int J Pharm Pharm Sci* 2016; 8 : 296-305.
- Kalra AV, Campbell RB. Mucin impedes cytotoxic effect of 5-FU against growth of human pancreatic cancer cells: overcoming cellular barriers for therapeutic gain. *Br J Cancer* 2007; 97 : 910-8.
- Wang P, Henning SM, Heber D. Limitations of MTT and MTS-based assays for measurement of antiproliferative activity of green tea polyphenols. *PLoS One* 2010; 5 : e10202.
- Malla RR, Gopinath S, Alapati K, Gorantla B, Gondi CS, Rao JS, *et al.* UPAR and cathepsin B inhibition enhanced radiation-induced apoptosis in gliomaintiating cells. *Neuro Oncol* 2012; 14 : 745-60.
- Anish N, Anitha M. *In silico* docking analysis of Janus kinase enzymes and phytochemicals. *J Chem Pharm Res* 2014; 6 : 493-9.

19. Kitchen DB, Decornez H, Furr JR, Bajorath J. Docking and scoring in virtual screening for drug discovery: Methods and applications. *Nat Rev Drug Discov* 2004; 3 : 935-49.
20. Perelman A, Wachtel C, Cohen M, Haupt S, Shapiro H, Tzur A, *et al.* JC-1: Alternative excitation wavelengths facilitate mitochondrial membrane potential cytometry. *Cell Death Dis* 2012; 3 : e430.
21. Malla RR, Gopinath S, Gondi CS, Alapati K, Dinh DH, Gujrati M, *et al.* Cathepsin B and uPAR knockdown inhibits tumor-induced angiogenesis by modulating VEGF expression in glioma. *Cancer Gene Ther* 2011; 18 : 419-34.
22. Graidist P, Martla M, Sukpondma Y. Cytotoxic activity of *Piper cubeba* extract in breast cancer cell lines. *Nutrients* 2015; 7 : 2707-18.
23. Hu W, Lee SK, Jung MJ, Heo SI, Hur JH, Wang MH, *et al.* Induction of cell cycle arrest and apoptosis by the ethyl acetate fraction of *Kalopanax pictus* leaves in human colon cancer cells. *Bioresour Technol* 2010; 101 : 9366-72.
24. Suryadinata R, Sadowski M, Sarcevic B. Control of cell cycle progression by phosphorylation of cyclin-dependent kinase (CDK) substrates. *Biosci Rep* 2010; 30 : 243-55.
25. Khuntawee W, Rungrotmongkol T, Hannongbua S. Molecular dynamic behavior and binding affinity of flavonoid analogues to the cyclin dependent kinase 6/cyclin D complex. *J Chem Inf Model* 2012; 52 : 76-83.
26. Graf F, Wuest F, Pietzsch J. Cyclin-dependent kinases (Cdk) as targets for cancer therapy and imaging. In: Gali-Muhtasib, editor. *Adv Cancer Ther*. Rijeka, Shanghai: Intech; 2011. p. 265-88.
27. Cover CM, Hsieh SJ, Tran SH, Hallden G, Kim GS, Bjeldanes LF, *et al.* Indole-3-carbinol inhibits the expression of cyclin-dependent kinase-6 and induces a G1 cell cycle arrest of human breast cancer cells independent of estrogen receptor signaling. *J Biol Chem* 1998; 273 : 3838-47.
28. Dwyer DJ, Camacho DM, Kohanski MA, Callura JM, Collins JJ. Antibiotic-induced bacterial cell death exhibits physiological and biochemical hallmarks of apoptosis. *Mol Cell* 2012; 46 : 561-72.
29. Zi X, Agarwal R. Silibinin decreases prostate-specific antigen with cell growth inhibition via G1 arrest, leading to differentiation of prostate carcinoma cells: Implications for prostate cancer intervention. *Proc Natl Acad Sci U S A* 1999; 96 : 7490-5.
30. Ly JD, Grubb DR, Lawen A. The mitochondrial membrane potential ($\Delta\psi(m)$) in apoptosis; an update. *Apoptosis* 2003; 8 : 115-28.
31. König A, Schwartz GK, Mohammad RM, Al-Katib A, Gabilove JL. The novel cyclin-dependent kinase inhibitor flavopiridol downregulates Bcl-2 and induces growth arrest and apoptosis in chronic B-cell leukemia lines. *Blood* 1997; 90 : 4307-12.
32. Druskovic M, Suput D, Milisav I. Overexpression of caspase-9 triggers its activation and apoptosis *in vitro*. *Croat Med J* 2006; 47 : 832-40.
33. Kim MH. Flavonoids inhibit VEGF/bFGF-induced angiogenesis *in vitro* by inhibiting the matrix-degrading proteases. *J Cell Biochem* 2003; 89 : 529-38.
34. Fotsis T, Pepper MS, Aktas E, Breit S, Rasku S, Adlercreutz H, *et al.* Flavonoids, dietary-derived inhibitors of cell proliferation and *in vitro* angiogenesis. *Cancer Res* 1997; 57 : 2916-21.

For correspondence: Dr Rama Rao Malla, Department of Biochemistry, GITAM (Deemed to be University), Visakhapatnam 530 045, Andhra Pradesh, India
e-mail: dr.rrmall@gmail.com